Regulation of recombination at yeast nuclear pores controls repair and triplet repeat stability

Xiaofeng A. Su,[1] Vincent Dion,[3,5] Susan M. Gasser,[3,4] and Catherine H. Freudenreich[1,2]

[1]Department of Biology, [2]Program in Genetics, Tufts University, Medford, Massachusetts 02155, USA; [3]Friedrich Miescher Institute for Biomedical Research, CH-4058 Basel, Switzerland; [4]Faculty of Natural Sciences, University of Basel, CH-4056 Basel, Switzerland

Secondary structure-forming DNA sequences such as CAG repeats interfere with replication and repair, provoking fork stalling, chromosome fragility, and recombination. In budding yeast, we found that expanded CAG repeats are more likely than unexpanded repeats to localize to the nuclear periphery. This positioning is transient, occurs in late S phase, requires replication, and is associated with decreased subnuclear mobility of the locus. In contrast to persistent double-stranded breaks, expanded CAG repeats at the nuclear envelope associate with pores but not with the inner nuclear membrane protein Mps3. Relocation requires Nup84 and the Slx5/8 SUMO-dependent ubiquitin ligase but not Rad51, Mec1, or Tel1. Importantly, the presence of the Nup84 pore subcomplex and Slx5/8 suppresses CAG repeat fragility and instability. Repeat instability in *nup84*, *slx5*, or *slx8* mutant cells arises through aberrant homologous recombination and is distinct from instability arising from the loss of ligase 4-dependent end-joining. Genetic and physical analysis of Rad52 sumoylation and binding at the CAG tract suggests that Slx5/8 targets sumoylated Rad52 for degradation at the pore to facilitate recovery from acute replication stress by promoting replication fork restart. We thereby confirmed that the relocation of damage to nuclear pores plays an important role in a naturally occurring repair process.

[*Keywords*: CAG repeats; chromosome fragility; repeat expansion; nuclear pore; Slx5/Slx8; nuclear organization]

Supplemental material is available for this article.

Received November 25, 2014; revised version accepted April 10, 2015.

DNA replication and DNA repair occur in the context of a spatially organized nucleus. In species ranging from yeast to humans, DNA repair events have been seen to occupy discrete foci. Most strikingly, recalcitrant or persistent DNA double-strand breaks (DSBs) in budding yeast were shown to relocate to the periphery of the nucleus (Nagai et al. 2008; Kalocsay et al. 2009; Oza et al. 2009), as did short telomeres engaged in recombinational repair (Khadaroo et al. 2009). Following relocation, DSBs became more constrained in their subdiffusive movement due to interaction with either nuclear pores or the inner nuclear membrane protein Mps3 (Nagai et al. 2008; Oza et al. 2009; Dion and Gasser 2013; Horigome et al. 2014). Exactly what is achieved by having distinct sites of interaction is unknown.

The types of damage for which such perinuclear sequestration was demonstrated in yeast are uncommon. Most commonly studied are DSBs induced by the HO endonuclease, which are difficult to repair for two reasons. First, homologous recombination (HR) is impaired because the usual donor for recombination, the sister chromatid, is also cut. Second, if the damage is repaired by precise end-joining, the site will be recleaved. When HR donor sequences are present on a nonhomologous chromosome, the HO-induced DSB undergoes extensive resection (30 kb) before shifting to the periphery (Oza et al. 2009). On the other hand, spontaneous HR foci in S-phase cells, which arise from recombination between sisters, are not enriched at the nuclear periphery, nor are replication forks stalled by dNTP depletion (Nagai et al. 2008; Bystricky et al. 2009; Oza et al. 2009; Dion et al. 2013). Thus, it has remained unresolved whether damage relocation to pores is a natural process in yeast and, if so, which physiological repair structures trigger recruitment to the nuclear envelope.

To address this, we undertook the study of a naturally occurring barrier to replication; that is, non-B DNA

[5]**Present address: Center for Integrative Genomics, University of Lausanne, CH-1015 Lausanne, Switzerland.**
Corresponding author: catherine.freudenreich@tufts.edu
Article published online ahead of print. Article and publication date are online at http://www.genesdev.org/cgi/doi/10.1101/gad.256404.114.

structures, such as the hairpins formed by certain trinucleotide repeats. It is well established that long CAG/CTG tracts (abbreviated CAG) interfere with DNA replication by stalling forks (Samadashwily et al. 1997; Pelletier et al. 2003; Cleary et al. 2010; Liu and Leffak 2012) and enhancing fork reversal (Fouche et al. 2006; Kerrest et al. 2009). Moreover, hairpins that occur on the 5′ flap of an Okazaki fragment lead to unligatable nicks (Liu et al. 2004) that are subject to post-replication repair (Daee et al. 2007; House et al. 2014). Not surprisingly, CAG repeats also form fragile sites, generating DSBs at a low but detectable frequency in a repeat length-dependent manner (Freudenreich et al. 1998; Jankowski et al. 2000; Callahan et al. 2003). Thus, CTG or CAG hairpins interfere with normal replication and repair, generating a recalcitrant but natural type of DNA damage.

Triplet-induced damage frequently leads to changes in repeat length, a phenomenon of particular relevance to human health. CAG repeat expansions are at the root of several neurodegenerative and neuromuscular diseases, such as Huntington's disease (HD), various spinocerebellar ataxias (SCAs), and myotonic dystrophy (DM1) (Lopez Castel et al. 2010; McMurray 2010). The expansion and contraction of triplet repeats occur in both germline and somatic tissues, leading to variable degrees of penetrance of the disease phenotype (Lopez Castel et al. 2010; Dion 2014). Appropriate repair of CAG repeat-induced damage is vital to the cell, as proper repair can prevent further expansion and aggravation of the disease (McMurray 2010; Usdin et al. 2015). For HD and DM1, it was shown that intergenerational expansions often occur in spermatogonia undergoing premeiotic replication (Yoon et al. 2003; Savouret et al. 2004). Studies in both model systems and human cells confirm that expansions can occur during DNA replication (Kim and Mirkin 2013; Usdin et al. 2015). Although it is unclear what triggers repeat expansion during replication, one possibility is that fork stalling or fork collapse at the repeat tract provokes a repair process that generates repeat length changes.

Interestingly, expanded CAG repeats introduced into yeast or human cells induce a checkpoint response in a repeat length-dependent manner (Lin et al. 2010; Sundararajan and Freudenreich 2011), and mutation of checkpoint proteins increases triplet repeat instability and fragility (for review, see Voineagu et al. 2009; Usdin et al. 2015). Indeed, wild-type yeast cells bearing 70 or 155 CAG repeats showed reduced rates of cell division, with ~5% exhibiting a prolonged checkpoint arrest, suggesting that a subset of repeat-induced damage is difficult to repair. In a *rad52*Δ strain, 8% of cells with a CAG-70 tract and 23% of cells with a CAG-155 tract succumbed to a persistent arrest, which was accompanied by activation of the checkpoint kinase Rad53 (mammalian Chk2) (Sundararajan and Freudenreich 2011). Consistently, yeast cells with expanded CAG repeats exhibit an increased number of Rad52 repair foci (Gellon et al. 2011). These results suggest that cells with expanded CAG tracts require specialized recombination-based processes to recover from repeat-associated DNA damage.

Given that a significant fraction of repeat-containing cells experience checkpoint activation and that previous work has linked difficult to repair DNA damage with both checkpoint activation and perinuclear relocation, we asked whether expanded CAG repeat tracts also shift position and whether they require relocation for efficient repair. Replication barriers formed by DNA structures had not been previously analyzed for their subnuclear location. We found that expanded CAG tracts in budding yeast associate with nuclear pores in S phase. Furthermore, nuclear pore-associated factors play an important role in preventing both repeat fragility and CAG expansions and contractions. Different from long-lived DSBs, expanded CAG tracts do not bind the Mps3 nuclear envelope protein and remain only transiently associated with the Nup84 pore subcomplex in late S phase. In addition, nuclear pore components, including Nup84 and the pore-associated Slx5/8 sumo-dependent ubiquitin ligase (STUbL), help suppress CAG expansions by regulating HR. We propose that Slx5/8 suppresses genomic instability during acute replication stress at the repeat tract by promoting replication fork restart. One factor targeted by this regulation appears to be the sumoylated form of Rad52. Taken together, our results demonstrate that a naturally arising form of DNA damage can provoke movement to a distinct subnuclear compartment and that pore association is necessary for a repair pathway that minimizes genome instability.

Results

Expanded CAG repeats localize to the nuclear periphery in late S phase

To monitor their subnuclear location, CAG sequences containing 0, 15, 70, or 130 repeats were integrated 6.4 kb away from a *lacO* array on yeast chromosome 6. The two elements were spatially indistinguishable by microscopy yet were on opposite sides of a replication origin so as to not be replicated by the same fork. They were also placed far from telomere and centromere elements to avoid these specialized domains influencing the position of the tagged CAG locus (Fig. 1A; Taddei et al. 2010). The inserted sequence was visualized by the binding of GFP-LacI to the *lacO* array, and position was scored relative to the nuclear periphery by binning into three equal zones, as previously described (Fig. 1B; Meister et al. 2010). CAG-70 and CAG-130 are both expanded unstable alleles, whereas CAG-15 represents an unexpanded stable allele.

In G1 phase, the repeat locus was evenly distributed among the three zones regardless of CAG repeat size (Fig. 1C). However, in S phase, there was a significant bias for the two larger CAG arrays to localize to zone 1, and peripheral enrichment increased with repeat length ($P = 1.0 \times 10^{-4}$ for either CAG-70 or CAG-130 compared with CAG-0 by χ^2 analysis) (Fig. 1D; Supplemental Table S1). Relative to the no repeat (CAG-0) control, the repeat-specific zone 1 increase is 13% for CAG-70 and 18% for CAG-130. Notably, the no repeat control was

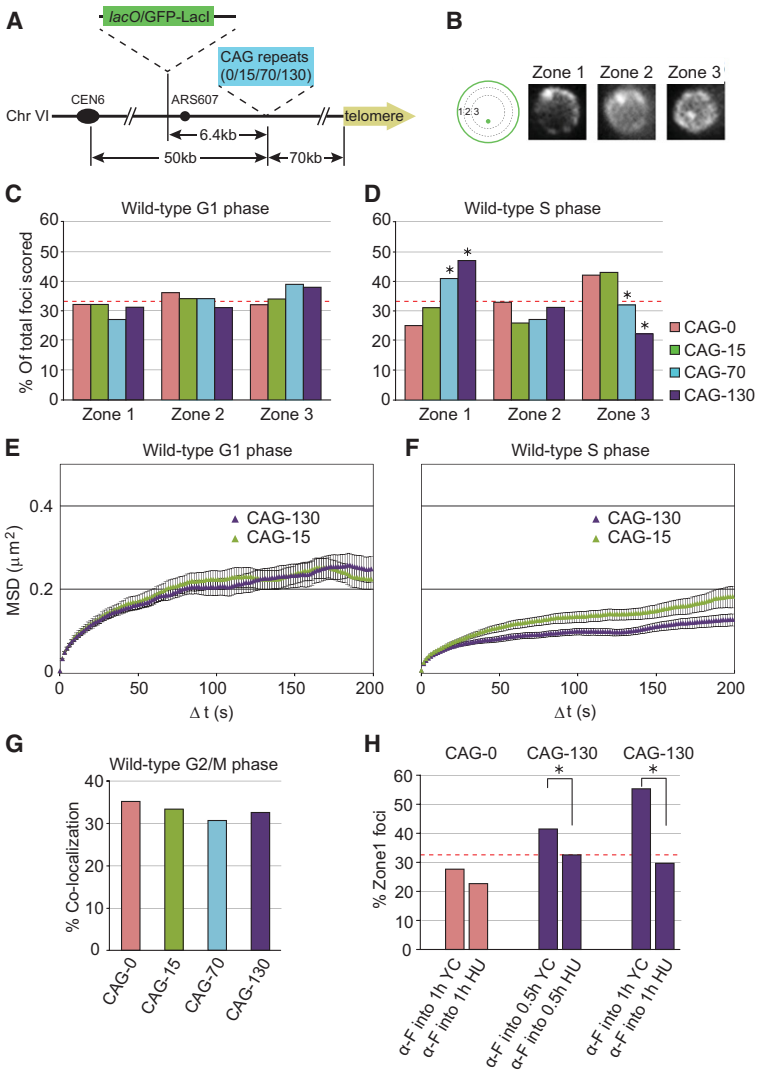

Figure 1. Expanded CAG repeats require replication to relocalize to the yeast nuclear periphery in S phase. (*A*) Organization of yeast chromosome VI containing integrated CAG repeats and a *lacO* array. (*B*) Example of zoning analysis. The nucleus was divided into three zones of equal volume, and the position of the focus was scored. (*C*,*D*) Zoning results in G1- and S-phase cells, identified by cellular morphology. (*) $P < 0.01$ compared with CAG-0 by χ^2 analysis ($P = 1 \times 10^{-4}$ for both CAG-70 and CAG-130). The number of cells analyzed (104–273), percentages, and *P*-values are listed in Supplemental Table S1. (*E*,*F*) Mobility of the CAG repeat in G1- and S-phase cells expressed as the mean square displacement distance (MSD) over the indicated time interval (Δt) for 12–21 cells (see the Materials and Methods, Supplemental Figure S1, Supplemental Table S2 for a detailed explanation and CAG-0, CAG-70, S-phase results). Vertical lines in black are the standard error for each time interval. (*G*) Percentage of GFP-LacI foci for large budded G2/M-phase cells with the indicated CAG repeat number that colocalizes with the nuclear periphery. $n = 54$, 129, 65, and 129 for CAG-0, CAG-15, CAG-70, and CAG-130, respectively. (*H*) Zone 1 CAG foci analyzed in S-phase cells 30 or 60 min after release from G1 arrest into the indicated medium; three-zone analysis was done as in *C* and *D*. (*) $P < 0.01$ compared with cells released into hydroxyurea (HU) medium by χ^2 analysis ($P = 4 \times 10^{-4}$ for 30 min and 1×10^{-4} for 60 min). The number of cells analyzed was 168–273 (for percentages and *P*-values, see Supplemental Table S1).

enriched in the innermost zone 3 in S-phase cells, indicating that the undamaged locus may prefer a central zone of the nucleus during replication.

To see whether the dynamics of the CAG repeat locus change with peripheral enrichment, the mobility of the GFP focus was tracked in living cells by taking a three-dimensional (3D) image stack at 1.5-sec intervals over periods of 5 min. This was followed by a mean squared displacement (MSD) analysis, which plots the square of the average distance a focus has traveled on one axis and increasing time intervals on the other (Supplemental Fig. S1A). This analysis has been useful to derive movement parameters (namely, the diffusion coefficient and the radius of constraint) of undamaged loci (Heun et al. 2001). It was subsequently used to show that movement increases at HO-induced DSBs (Dion et al. 2012; Mine-Hattab and Rothstein 2012) but not at spontaneously occurring repair foci (Dion et al. 2013). Movement analysis showed a significant decrease in mobility of the expanded repeat locus in S-phase cells (Fig. 1F). As with positioning, this decrease in mobility was repeat length-dependent, with CAG-15 and CAG-0 showing identical curves, and CAG-70 and CAG-130 progressively losing mobility (Fig. 1F; Supplemental Fig. S1B; Supplemental Table S2). The radii of constraint correspond to 14% of the nuclear volume for CAG-0 and 8% for CAG-130. No difference in mobility was scored between the two repeat sizes in G1-phase cells, where movement is significantly higher, as previously observed (Fig. 1E; Heun et al. 2001). These results are consistent with the expanded repeat locus being tethered to a perinuclear structure during S phase.

We followed the fate of the repeats at the periphery in S phase by determining whether the repeats remain peripheral in G2 phase. The nuclei of G2-phase cells are no longer spherical; thus, we were unable to use three-zone scoring accurately (Meister et al. 2010). Instead, we monitored colocalization of the tagged CAG foci with GFP-Nup49. Using >60% overlap as a cutoff for colocalization, we found that neither expanded CAG repeat tract remained peripheral in G2-phase cells (Fig. 1G). The loss of CAG-130's peripheral localization was not due to an overall loss of GFP-LacI foci in G2 cells: In >100 G2 cells analyzed,

96% of CAG-0 and 94% of CAG-130 cells contained foci, similar to S phase, where 97% of CAG-0 and CAG-130 cells contained foci. Thus, the shift of the expanded repeat tract to the periphery is a transient event in otherwise normal cycling cells that occurs in S phase and is resolved by G2. Both the high percentage of perinuclear foci scored and their transient nature argue that the initiating event of this relocation is a type of reparable damage.

To determine whether replication was required for relocation, cells were arrested in G1 and released into 0.2 M hydroxyurea (HU) to arrest replication forks within a few kilobases of the origin (Sogo et al. 2002; Cobb et al. 2003). Under these conditions, most forks should not traverse the CAG repeat, which lies 6 kb away from ARS607. Consistently, the increase in zone 1 localization was lost (Fig. 1H). This suggests that replication through the repeat is required for relocation. Given that hairpin-forming CAG tracts block replication forks, we speculate that aberrantly paused replication forks themselves lead to pore association, possibly reflecting a need to engage an alternate pathway for fork restart.

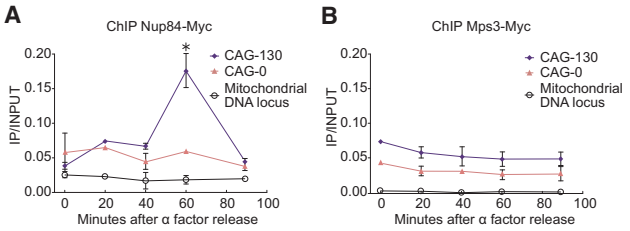

Figure 2. CAG Nup84 interaction occurs transiently in late S phase. Samples from Nup84-Myc (*A*) or Mps3-Myc (*B*) strains were immunoprecipitated with anti-Myc antibody. The level of qPCR DNA product 92 base pairs (bp) from the CAG repeat was compared with levels amplified from input DNA. Each time point is the mean of two experiments ± SEM. (*) $P = 0.002$ by ANOVA comparison of all CAG-130 time points; $P = 0.04$ by *t*-test compared with the same CAG-0 60-min time point. The mitochondrial *OLI1* locus that should not interact with the nuclear periphery provides a negative control.

CAG repeats interact with the nuclear pore component Nup84 but not with Mps3

Using chromatin immunoprecipitation (ChIP), it was shown that an irreparable DSB associates with the nuclear pore Nup84 subcomplex as well as with the Slx8 STUbL subunit by 2–4 h after HO induction (Nagai et al. 2008). Yeast Nup84 is part of a conserved Y-shaped, seven-subunit complex that forms the outer ring of the nuclear pore (Brohawn et al. 2009). Cells lacking Nup84 exhibit hypersensitivity to DNA-damaging agents MMS, bleomycin, and ionizing radiation (Bennett et al. 2001; Loeillet et al. 2005) and are defective in repair of subtelomeric breaks (Therizols et al. 2006). To determine whether the expanded CAG repeats bind nuclear pores, we immunoprecipitated chromatin with an antibody to Myc-tagged Nup84 and quantified the level of associated CAG-0 or CAG-130 repeat DNA. CAG-130 DNA was transiently enriched in Nup84-associated DNA by 60 min after release from G1, whereas the CAG-0 control was not (Fig. 2A). This correlates with the repositioning scored in the three-zone assay and is consistent with the notion that CAG-induced replication fork damage leads to an interaction with the nuclear pore. Flow cytometry and cell morphology analysis both indicated that the cells were in late S phase at the 60-min time point at which Nup84 interaction was observed (Supplemental Fig. S2). In this experiment, we used strains lacking the nearby *lacO* array to confirm that peripheral localization of the repeat tract (Fig. 1D) is not an artifact of having the *lacO* array in proximity.

To see whether the inner nuclear envelope protein Mps3 was also involved in CAG-130 binding, we performed a similar ChIP experiment for Myc-tagged Mps3. No enrichment for the CAG repeat was scored in any phase of the cell cycle (Fig. 2B). The low but significant signal for Mps3 with the chromosome 6 locus when compared with a mitochondrial locus likely reflects random contact with the periphery, as observed in the zoning assays. This suggests that a cell cycle-specific increase in Mps3 would have been detectable were it to occur.

CAG repeats exhibit increased fragility and instability in the absence of Nup84 or Slx5/8, with instability occurring during Rad52-dependent recombination

Two questions arise from these observations: First, why do expanded repeats localize to the nuclear pore? Second, what is the consequence of interrupting this interaction? To address these questions, we monitored fragility and instability of an expanded CAG repeat (CAG-70) in backgrounds mutant for the pore-associated proteins using two previously established assays (Fig. 3A,B; see the Materials and Methods; Callahan et al. 2003; Sundararajan et al. 2010). Deletion of Nup84 led to a dramatic increase in fragility that was not limited to repeat DNA (Fig. 3C; Supplemental Table S3). The Nup84 complex is an important component of the nuclear pore, and spontaneous gross chromosomal rearrangement (GCR) rates increase in its absence (Nagai et al. 2008); thus, its functions are not expected to be limited to lesions occurring at the CAG repeat. Nonetheless, fragility in the *nup84*Δ strain was further exacerbated by the presence of the repeat, indicating that repeat-induced damage is either increased or less efficiently repaired in the absence of Nup84.

The Slx5/Slx8 complex (Ii et al. 2007; Xie et al. 2007) was shown previously to colocalize with nuclear pores and bind to Nup84 (Nagai et al. 2008). Mutants lacking Slx5 or Slx8 spontaneously accumulate Rad52 foci and show increased rates of ectopic recombination (Burgess et al. 2007). They also show increased Mec1/Ddc2 repair foci, GCRs, and hypersensitivity to DNA-damaging agents (for review, see Nagai et al. 2011). In our case, *slx5* or *slx8* mutants did not show a marked effect on fragility in the absence of CAG repeats but significantly increased fragility of a CAG-70-containing YAC ($P < 0.05$) (Fig. 3C; Supplemental Table S3). Thus, we propose that both the Nup84 pore complex and the Slx5/8 STUbL are important to either prevent chromosome breakage at the CAG repeat or process such lesions rapidly.

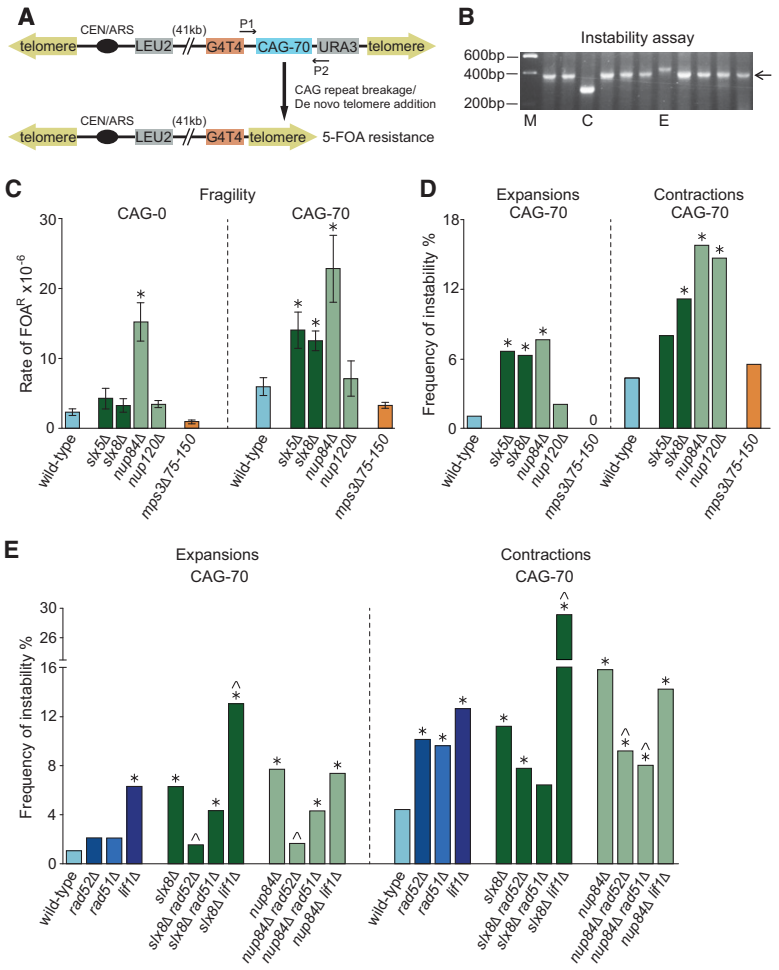

Figure 3. CAG fragility and instability are increased in strains deleted for Nup84 or Slx5/8; expansions are dependent on Rad52. (*A*,*B*) Assay for CAG fragility (*A*) and instability (*B*). The arrow indicates the size of the CAG-70 repeat PCR product. (C) Contraction; (E) expansion; (M) marker. (*C*) Rate of $FOA^R \times 10^{-6}$ in the indicated mutants. (*) $P < 0.05$ compared with wild type by *t*-test. The average of at least three experiments ± SEM is shown (see also Supplemental Table S3). (*D*,*E*) CAG-70 expansion and contraction frequencies in the indicated mutants. (*) $P < 0.05$ compared with wild type; (^) $P < 0.05$ compared with the *left*-most single mutant of each group, by Fisher's exact test (see also Supplemental Table S4).

Whereas chromosome fragility indicates a failure of repair, repeat instability can happen during a productive DNA repair process; we note that expansions and contractions of a CAG-70 tract occur at a high frequency even in wild-type yeast cells (~1% expansion and 5% contractions) (Fig. 3D). Notably, the deletion of *nup84*, *slx5*, or *slx8* led to a further and significant increase in both CAG expansions and contractions (Fig. 3D; Supplemental Table S4), indicating that the fidelity of either DNA synthesis or repair is compromised in these backgrounds. Deletion of another component of the Nup84 complex, Nup120, increased contractions but not expansions or fragility. In contrast, an N-terminal deletion of Mps3 that results in loss of DSB association to the nuclear periphery (Oza et al. 2009; Horigome et al. 2014) did not affect either CAG fragility or instability. This is consistent with the lack of CAG repeat interaction with Mps3 by ChIP (Fig. 2B). Taken together, our data show that Nup84 and Slx5/8 both contribute to proper repair of replication-induced damage at an expanded CAG repeat during its transient association with the nuclear periphery.

To better understand the process that occurs at the nuclear pore to prevent repeat expansions, we deleted other repair proteins in the *nup84* and *slx8* backgrounds and scored for repeat expansions or contractions. Deletion of the HR protein Rad52 suppressed the increased rate of CAG expansions in both *nup84* and *slx8* backgrounds, while deletion of *lif1*, a cofactor for Ligase 4 that participates in end-joining reactions, not only produced expansions and contractions on its own but aggravated the *slx8* defect (Fig. 3E). Removal of Rad51 partially suppressed the expansions observed in *slx8*- or *nup84*-deficient cells (Fig. 3E; Supplemental Table S4). In the case of contractions, the loss of either Rad52 or Rad51was deleterious, provoking enhanced contractions, yet this effect was largely epistatic with either *slx8* or *nup84* mutation (Fig. 3E). This places the CAG instability observed in either *slx8* or *nup84* cells in a pathway that involves the machinery of HR, while it is additive with compromised nonhomologous end-joining (NHEJ). Indeed, the absence of the nuclear pore Nup84 protein or its binding partner, Slx8, led to CAG expansions in a manner fully dependent on Rad52 and partially dependent on Rad51.

Slx5/8 and Nup84, but not Rad51, Rad52, Mec1, or Tel1, are required for CAG peripheral localization

To correlate the relocation event with the CAG fragility and instability observed in the *slx5* and *slx8* mutants, we next asked whether Slx5/8 is required for the

localization of the expanded repeat tract to the nuclear periphery. Indeed, we found that the enrichment in peripheral zone 1 CAG-130 foci was abolished in the *slx5* background (Fig. 4A). Given the importance of this finding, we confirmed the result using a different assay, colocalization of an RFP-tagged CAG-130 locus with the nuclear periphery, and observed that colocalization was significantly reduced in an independent *slx5Δ* mutant (Fig. 4B). The earlier report that found an insignificant effect of *slx5*Δ on DSB relocation to the nuclear periphery (Nagai et al. 2008) most likely reflects the fact that DSBs bind Mps3 as well as nuclear pores, unlike expanded CAG repeats (Figs. 2B, 4A). We also observed the loss of hyperconstrained mobility of the CAG-130 tract in the *slx5* strain (cf. Figs. 1F and 4C), further confirming that the Slx5/8 complex is required to tether the expanded CAG tract to the nuclear pore. We were not able to accurately score the location of the CAG tract in the *nup84*Δ or *nup120*Δ strains using the zoning assay because nuclear shape is distorted in these backgrounds, and there is a partial clustering of the pores (for examples, see Supplemental Fig. S3A). However, using an assay that scores colocalization with pores, we observed a reduced association of the CAG-130 tract with nuclear pores in both the *slx5* and *nup84* deletion strains in S phase (Fig. 4B). Taken together, our data indicate that forks stalled at the expanded CAG tract move to the nuclear pore in a manner that is dependent on the Slx5/8 STUbL complex and Nup84. We cannot distinguish whether they are important for the recruitment or the maintenance of the interaction. Nonetheless, this identifies a role for the Slx5/8 complex in tethering a natural replication fork barrier to the nuclear pore transiently in late S-phase cells.

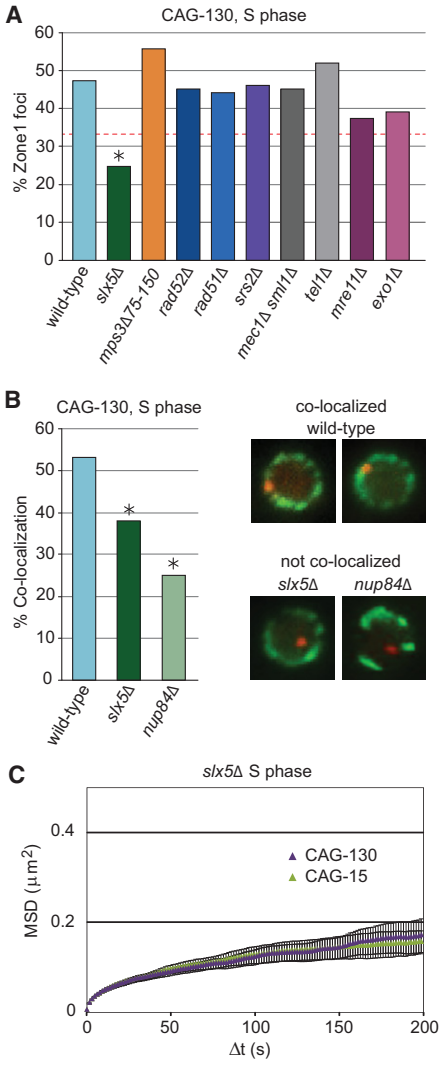

Figure 4. Slx5 and Nup84 are required for CAG peripheral localization and reduced mobility. (*A*) Percentage of CAG-130 tracts in zone 1 during S phase for the indicated strains. (*) $P < 0.01$ compared with wild-type CAG-130 by χ^2 analysis ($P = 1 \times 10^{-4}$ for *slx5*Δ compared with wild type). For the number of cells analyzed (98–147), percentages, and *P* values, see Supplemental Table S1. (*B*) Colocalization analysis of RFP-LacI CAG-130 foci with the GFP-Nup49-stained nuclear pore. Representative images are shown. $n = 178$ for wild type; $n = 126$ for *slx5*Δ; $n = 126$ for *nup84*Δ; (*) $P \leq 0.01$ compared with wild type by Fisher's exact test. (*C*) MSD analysis in the *slx5*Δ mutant, analyzed as in Figure 1.

Earlier work showed that the DNA damage checkpoint, end resection, and HR factor Rad51 or Rad52 were differentially required for relocation to the nuclear periphery, depending on the phase of the cell cycle and the anchorage site (Nagai et al. 2008; Kalocsay et al. 2009; Horigome et al. 2014). We therefore tested whether the CAG-130 repeat requires the activity of the Mec1 or Tel1 checkpoint kinases for relocation. Surprisingly, neither function was necessary for the peripheral recruitment of the CAG-130 tract in S-phase cells (Fig. 4A), and relocation was not significantly altered by the loss of Rad52, Rad51, or the Srs2 protein, which controls Rad51/Rad52-dependent recombination and CAG repeat stability (Kerrest et al. 2009; Marini and Krejci 2010). Consistently, recent results showed that DSBs are still enriched at the periphery in *rad51*Δ and *rad52*Δ mutants in G1 and S phase, suggesting that a Rad51-independent binding site also exists for DSBs (Horigome et al. 2014). Thus, the Slx5/8 complex does not require the Rad51, Rad52, Mec1, or Tel1 protein to tether the CAG repeat.

Given that that the deletion of either Mre11 or Exo1 increases CAG fragility and expansions (Sundararajan et al. 2010), that Mre11 binds expanded CAG repeats in early S phase (Sundararajan and Freudenreich 2011), and that Mre11 and Exo1 bind and process stalled forks (Tittel-Elmer et al. 2009; Tsang et al. 2014), we also tested the role of these proteins in CAG tract relocation. The results on CAG-130 positioning are intermediate between those in wild type and *slx5*Δ cells (Fig. 4A). Unlike in wild-type cells, the CAG-130 tract exhibited a random distribution in *mre11*Δ and *exo1*Δ cells, although the difference from wild type did not reach statistical significance ($P = 0.08$ and $P = 0.1$, respectively) (Supplemental Table S1). Whereas this suggests that resection may facilitate pore association during CAG-130-induced damage, we cannot rule out indirect effects of either mutation on replication that might impair the stalling or relocation events to generate this intermediate result.

Sumoylation of Rad52 helps suppress CAG repeat instability, and its Slx8-dependent degradation coincides with fork stalling and pore relocation

Given the enzymatic activity of the Slx5/8 complex, it could act by ubiquitinating Rad52 or other sumoylated repair proteins involved in the control of HR and targeting them for degradation. To test this idea, we asked whether CAG instability was affected by the mutation of sumoylatable lysines to arginines in Rad52, Rad59, or Srs2 protein using characterized *rad52-3KR*, *rad59-2KR*, and *srs2-3KR* mutants (Sacher et al. 2006; Altmannova et al. 2010; Saponaro et al. 2010). Although mutation of Rad59 or Srs2 had no effect, CAG expansions and contractions were increased in the *rad52-3KR* strain to the same level as in a *slx8* mutant (Fig. 5A). Moreover, the double mutant exhibited similar levels of instability, consistent with the two proteins working in the same pathway (Fig. 5A).

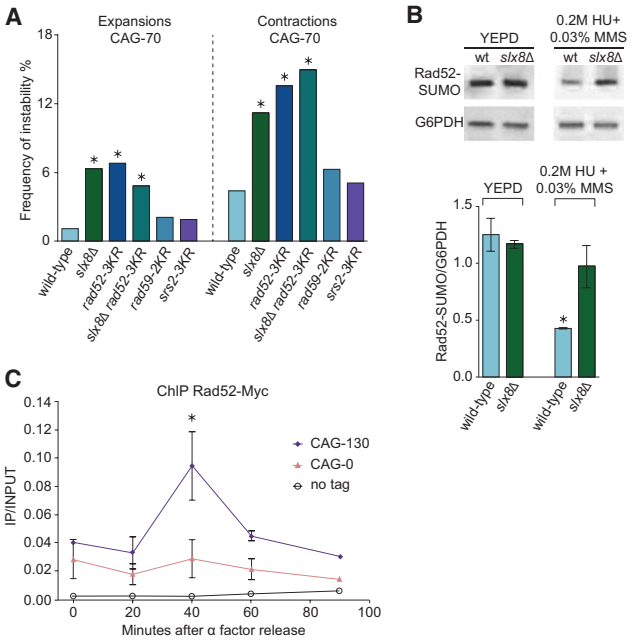

Figure 5. Rad52 dynamics at collapsed forks and pore-localized CAG-130 repeats. (*A*) Rad52 sumoylation is required to prevent CAG-70 instability. Instability analysis was as in Figure 3. (*) $P < 0.05$ compared with wild type by Fisher's exact test. (KR) Lysine-to-arginine mutations that eliminate modification by SUMO. (*B*) Western blot analysis of a Rad52-SMT3ΔGG-13Myc fusion protein in wild-type and *slx8*Δ strains grown in rich (YEPD) medium without or with 0.2 M HU + 0.03% MMS. The average of two experiments was quantified using National Institutes of Health ImageJ. The standard error is shown. (*) $P = 0.03$ by *t*-test compared with wild type in YEPD medium. The difference between *slx8*Δ strains grown in the two conditions is not significant. $P = 0.41$. (*C*) Enrichment of Rad52-Myc at the CAG-130 or CAG-0 locus in wild-type strains. ChIP analysis was as in Figure 2. (*) $P = 0.06$ by ANOVA comparison of all CAG-130 time points. Normalization to the *ACT1* locus in the same samples showed the same profile, with CAG-130 significantly higher than CAG-0 at 40 min, $P = 0.012$ by one-way ANOVA (data not shown). Immunoprecipitation/input for the CAG-130 strain with untagged Rad52 (no tag) shows that the antibody pull-down is specific to the Rad52-Myc protein.

If sumoylated Rad52 is targeted for degradation by the Slx5/8 STUbL, then one might expect that Rad52-SUMO would accumulate in a *slx5/8* mutant background. Sumoylated Rad52 is in low abundance, yet previous studies were able to detect sumoylated Rad52 after high-dose (0.3%) MMS treatment (Sacher et al. 2006; Burgess et al. 2007). To specifically observe the fate of sumoylated Rad52 in our strain background, we used a Rad52-SMT3 fusion protein (referred to here as Rad52-SUMO) and detected levels in either rich medium or a combination of 0.2 M HU and a low dose of MMS (0.03%) to mimic the conditions that were shown to result in collapsed forks and origin relocation to zone 1 (Nagai et al. 2008). Under these conditions, a reproducible and statistically significant decrease in Rad52-SUMO was observed in wild-type cells but not in the *slx8*Δ strain (Fig. 5B). These data are consistent with the idea that sumoylated Rad52 is targeted for degradation by the Slx5/8 STUbL under conditions that result in collapsed forks, such as those provoked by CAG-130.

We also investigated the colocation of Rad52 foci with the CAG-130 repeat. Rad52 foci have been shown to occur at DSBs and broken/collapsed forks but not at forks stalled with HU (Lisby et al. 2004). Even though 36% of spontaneous Rad52-YFP foci in a strain containing CAG-130-RFP colocalized with the repeat tract, the vast majority of the peripheral CAG-130 foci in S-phase cells did not colocalize with a Rad52 focus (only three of 95 [3.2%]) (Supplemental Table S6). This experiment was done in fixed cells; thus, some short-lived Rad52 foci may not have been detected. Nonetheless, it suggests that most CAG repeats located at the nuclear pore in wild-type cells do not contain long-lived damage that accumulates Rad52 to the levels needed for focus visualization, further supporting the idea that the majority of damage at pore-associated CAGs in wild-type cells does not entail DSBs but rather reflects compromised replication forks. However, in *slx8*Δ cells, even though significantly fewer CAG-130 tracts were localized to the periphery, a greater percentage of peripheral CAG foci colocalized with Rad52 (10 of 49 [20%] for *slx8*Δ vs. 3% for wild-type; $P = 1.2 \times 10^{-6}$) (Supplemental Table S6). These data support the conclusion that Slx5/8 targets Rad52 for degradation when it is bound to a CAG-130 tract located at the nuclear pore. To investigate this hypothesis in another manner, we quantified the level of Rad52 protein at the CAG-130 repeat (or CAG-0 control) by ChIP over the course of a cell cycle. In wild-type cells, Rad52 levels were elevated at the CAG-130 repeat compared with the no repeat control at 40 min into S phase; however, by 60 min, when the repeat was interacting with the pore, the level decreased (Fig. 5B). These data are consistent with the idea that a portion of Rad52 is removed when the CAG-130 tract associates with the nuclear pore.

Discussion

Forks stalled by HU do not bind nuclear pores, but treatment with both HU and MMS, conditions that enhance

fork collapse, does lead to pore enrichment (Nagai et al. 2008). Based on this, it was proposed that pore association helps resolve DNA damage at collapsed forks. Expanded CAG repeats represent a natural fork barrier similar to other barriers found in higher eukaryotic cells, which contain many structure-forming sequences in their genomes. Our data show that nuclear pore association can be a transient event during S phase and is not restricted to irreparable DSBs or conditions of severe DNA damage. Indeed, the replication dependence of pore association and high survival rate of CAG-130-containing cells argues that the relocation of this locus to the nuclear pore may be a normal part of the repair process for fork-associated lesions. The CAG-associated event that provokes pore association is likely a fork that has failed to replicate through a hairpin structure, thus necessitating the engagement of an alternate pathway to restart replication. Alternatively, in some cases, the replisome may have bypassed the hairpin, leaving damage behind the fork to be repaired by recombination. Rad51/52-dependent fork restart occurs at a protein-mediated fork barrier (Lambert et al. 2005, 2010) as well as at reversed forks or uncoupled forks containing long ssDNA regions, which are induced by sublethal genotoxic treatments (Zellweger et al. 2015). Thus, the fork relocation event characterized here for expanded CAG repeats could apply to other fork barriers as well.

There are several differences between the interaction of the CAG-130 repeat with the nuclear periphery and the interactions reported for DSBs. The interaction observed for the CAG tract is transient and occurs only in S phase, not G1 or G2. In strains lacking a donor for repair, induced DSBs associate with the nuclear pore in both G1 and S phase and with Mps3 in S phase, persisting for 2–5 h in some cases following extensive end resection (Nagai et al. 2008; Oza et al. 2009; Horigome et al. 2014). We speculate that this difference correlates with the fact that the DSBs are not repaired, while the CAG-130 damage is in most cases. In addition, the CAG tract appears to interact only with the pore and not the Mps3 protein of the inner nuclear envelope, and pore association persisted in the absence of the Mec1 or Tel1 kinases or the Rad51/Rad52 repair proteins, again contrasting with induced DSBs that require Mec1 and Rad51 for peripheral accumulation in S phase (Nagai et al. 2008; Kalocsay et al. 2009; Oza et al. 2009).

Altogether, our data suggest that a collapsed fork is the initial structure that provokes relocation of the expanded CAG repeats to the pore. This conclusion is supported by the fact that the two proteins found to be required for relocation of the CAG tract (Nup84 and Slx5/8) act to prevent breakage at the repeat. Also, the level of relocation was not increased in mutants that increase breaks at the repeat (i.e., *rad51*, *rad52*, *srs2*, *mec1*, *mre11*, and *exo1*) (see Fig. 5A; Lahiri et al. 2004; Kerrest et al. 2009; Sundararajan et al. 2010) or in G2, when breaks would be expected to occur, suggesting that an unbroken but inactive fork is the relevant damage. However, the exact nature of the collapsed fork is unclear: Presumably, the replisome is not intact or fully functional, as an alternative replication restart pathway is required. The DNA may contain unreplicated gaps due to the inability to replicate through CAG or CTG hairpins, reversed forks or other template switch intermediates, or a one-ended DSB, all of which have been invoked at trinucleotide repeats (Fig. 6; for review, see Mirkin 2006; Kim and Mirkin 2013; Usdin et al. 2015). Because treatment with HU does not lead to peripheral association (Fig. 1H; Nagai et al. 2008), the structure at the CAG tract that provokes pore relocation cannot simply be a stalled fork but one that has undergone a transition of either the DNA structure or the protein components bound to the fork.

We suggest that the forks that are unable to efficiently resume replication get shunted to the nuclear pore to be restarted in a manner that normally prevents chromosome breakage and repeat instability (Fig. 6). Rad51/52-dependent fork restart has been shown to occur in the absence of chromosome breakage at a protein-mediated fork barrier in fission yeast, with resumption of replication occurring within S phase, similar to the situation here (Mizuno et al. 2009). At this strong protein-mediated barrier, Rad51 and Rad52 were detected at the stalled fork by ChIP (Tsang et al. 2014). In mammalian cells, Rad51 is also associated with forks stalled by low doses of replication inhibitors that exhibit ssDNA gaps and fork reversal but no increase in DSBs (Zellweger et al. 2015). Thus, the increase of Rad52 binding at the CAG-130 tract observed in mid-S phase could represent Rad51/52 binding to the stalled fork before it relocates to the pore.

Our data show that the Slx5/8 STUbL is needed to tether the CAG-130 repeat to the pore and that a Rad52-dependent repair process is modulated by the Slx5/8 complex. Since the Slx5/8 STUbL is a key part of this process, we propose that degradation of a regulatory protein or proteins by the proteasome after SUMO-targeted ubiquitin ligation facilitates fork restart or high-fidelity repair. Our data indicate that one of the key targets of Slx5/8 could be the sumoylated form of Rad52 itself. Other repair proteins are also sumoylated and could be targets in addition to Rad52. For example, a recent study showed that Sgs1 foci are reduced after HU treatment in a Slx8-dependent manner (Bohm et al. 2015). At a protein-mediated stall, the restarted fork was more prone to replication slippage, producing deletions (Iraqui et al. 2012). A similar fork restart mechanism could be occurring at the CAG repeat, contributing to the low level of instability, biased toward contractions, that is observed in unperturbed wild-type cells (Fig. 6, successful restart pathway). Alternatively, other pathways could be involved in creating instability in wild-type cells as long expanded repeats cause a low level of DSBs and checkpoint arrest even when repair and checkpoint pathways are intact (Sundararajan et al. 2010; Sundararajan and Freudenreich 2011).

In the absence of pore association, more breakage at the CAG repeat was observed, suggesting that this restart system was no longer functioning, and the collapsed fork was converted to a DSB (Fig. 6, failed restart pathway). In addition, a Rad52-dependent process occurs that is more likely to result in repeat expansions and contractions (Fig. 3). This alternate pathway could be break-induced replication (BIR), single-strand annealing (SSA), or both, two pathways of recombination that are more dependent on Rad52 than

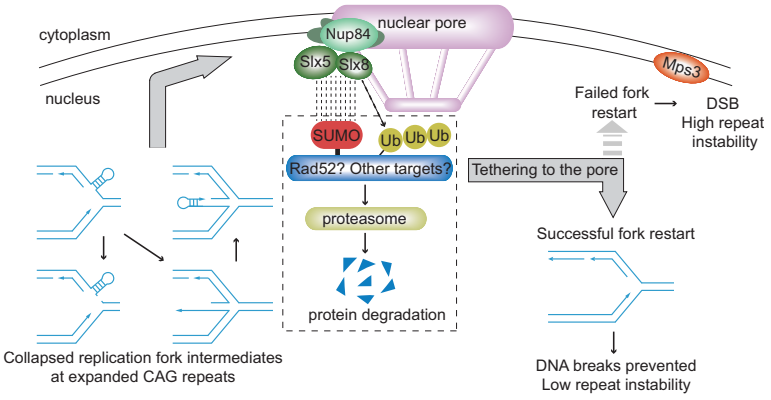

Figure 6. Model for the role of transient tethering of expanded CAG repeats to the nuclear periphery in late S phase. Expanded CAG tracts form hairpin structures that interfere with replication and stall replication forks. We propose that some stalled forks, especially for longer CAG-130 repeats, are not able to proceed; in this case, the replisome may be dissociated or modified to create a "collapsed" fork with or without a DNA break. Fork reversal may occur, as has been proposed (Mirkin 2006) and shown for CAG and GAA triplet repeats (Fouche et al. 2006; Kerrest et al. 2009; Follonier et al. 2013). Note that a lagging strand hairpin is shown initiating the fork reversal, but it could also occur by a leading strand hairpin; in this case, replication through some of the repeats would be needed for the repeat sequence to be part of the regressed arm of the fork. Rad51/52 could bind the gap, the reversed fork end, or a one-ended break. (*Left* side) One or more of these structures is recruited to the nuclear pore in a manner dependent on the Nup84 nucleoporin and the Slx5/8 STUbL. (*Middle* box) At the pore, Slx5/8 interacts with sumoylated Rad52 (and potentially other targets) bound to the fork and adds ubiquitin to target it for degradation by the proteasome. (*Right*) This process facilitates successful fork restart by nonsumoylated Rad52, preventing breakage; expansions or contractions could occur during recovery but are minimized (downward arrow). Alternatively, if this process fails, the fork may break or be cleaved by a nuclease to produce a DSB, which is then repaired by low-fidelity HR (e.g., single-strand annealing [SSA] or break-induced replication [BIR]) or NHEJ in a process more likely to generate repeat length changes, especially contractions (upward arrow).

on Rad51. Both pathways increase in *slx5* or *slx8* cells (Burgess et al. 2007). Consistently, GCRs also increase in *slx5* mutants (Nagai et al. 2008; Oza et al. 2009), suggesting that a repair mechanism that is prone to creating genome rearrangements is at work in this background. Sumoylated Rad52 constitutes the minority of the Rad52 proteins in the cell (Altmannova et al. 2010; Esta et al. 2013); thus, degradation of only this form would still leave unmodified Rad52 available for mediating recombination. Sumoylated Rad52 exhibits reduced mediator activity in Rad51 filament formation compared with the nonsumoylated form (Esta et al. 2013). Conversely, the nonsumoylatable Rad52-3KR protein causes increased recombination within the rDNA and at direct and inverted repeats (Altmannova et al. 2010). Thus, failure to regulate or degrade the sumoylated form of Rad52 could alter HR outcomes, for example, by decreasing Rad51-mediated fork restart and increasing Rad52-mediated SSA to cause contractions at the CAG repeat that were prominent in both *nup84* and *slx5/8* mutants. There are clearly multiple pathways that suppress repeat expansion and contraction in yeast, as the ablation of Lif1, a cofactor of the NHEJ-involved ligase 4, also leads to expansions and contractions. The latter, however, are additive with mutations of *SLX5/8* and *NUP84*, while the effects of *rad52* deletion either suppress or are epistatic with the pore-associated pathway of repair.

In summary, we observed that an expanded CAG repeat tract transiently relocates to nuclear pores in late S phase in a manner dependent on replication. This shows for the first time that naturally occurring, replication-dependent damage relocates to the nuclear pore for repair or fork recovery. The interaction of the CAG repeat with the pore is necessary to suppress chromosome breakage and prevent instability of the repeat tract. Our data go beyond studies that have shown the localization of induced DSBs with the nuclear periphery in yeast and suggest that the repositioning of damage within the nucleus is an integral part of an accurate recombinational repair and fork restart pathway. We identified degradation of sumoylated Rad52, a target of the Slx5/8 STUbL, as one component of the repair pathway regulation that occurs at the nuclear pore. Importantly, we show that sumoylated Rad52 is lost from collapsed forks in a Slx8-dependent manner (Fig. 5B), and the reduction of Rad52 at the CAG-130 tract correlates with the time at which association of the CAG repeat with pores peaks (Fig. 5C). These data argue for a model in which relocation facilitates the eviction or degradation of a modified form of Rad52, which leads to fork recovery and avoidance of DSBs and associated genome instability.

In mammalian cells, maintenance of telomeres by the recombination-dependent ALT pathway also occurs at a particular nuclear structure, the PML body (Yeager et al. 1999), which harbors RNF4, the homolog of Slx5/8 (Nagai et al. 2011). RNF4 has also been implicated in the response to DNA damage and facilitates damage-induced HR in human cells (Galanty et al. 2012; Yin et al. 2012; Ragland et al. 2013). Moreover, DSBs in heterochromatin have been shown to move out of heterochromatin for repair in *Drosophila* and human cells (Chiolo et al. 2011; Jakob et al. 2011), and DSB repair pathway choice is also influenced by nuclear position in human cells, with end-joining more prevalent at the nuclear lamina, and HR more prevalent at nuclear pores (Lemaitre et al. 2014). Thus, the regulation of recombination and repair outcome through nuclear relocation may be a general mechanism that is conserved from yeast to humans.

Materials and methods

Yeast strains and methods

All yeast strains used in this study are listed in Supplemental Table S7. CAG-70 or CAG-130 repeats were inserted into a yeast

chromosome XI noncoding region upstream of the tA(AGC)F gene, 6371 base pairs (bp) from the *lac* operator array when present, such that the CAG strand is on the lagging strand template. All repeat sizes were confirmed by PCR sizing and sequencing. Yeast knockout and point mutations were created by one-step gene replacement or by crossing the CAG repeat containing YAC into the parent strain and were confirmed by PCR or PCR and sequencing for point mutants. Rad52-SMT3ΔGG (M. Lisby) was tagged with 13 Myc at its endogenous locus and verified by PCR and Western blot analysis. Details of strain construction and parent strains are in the Supplemental Material. CAG tract length was reverified in all starting colonies used for all of the assays described below.

Zoning, mobility, and colocalization analysis

Cells from colonies with the desired CAG length were grown to 5×10^6 cells per milliliter. For zoning, cells were fixed using 4% paraformaldehyde. Z-stack pictures were captured, images were deconvolved, and three-zoning criteria was used to evaluate the location of GFP foci for G1- and S-phase cells as described in the Supplemental Material. For colocalization experiments in G2/M-phase cells, a CAG-GFP focus overlapping by ≥60% with the GFP-Nup49 ring was determined as at the periphery. Chromatin mobility assays were done as in Dion et al. (2013) and described in detail in the Supplemental Material. Cell cycle phase was determined by yeast morphology and bud size.

Analysis of CAG repeat fragility and instability

The CAG tract was amplified from yeast colonies using primers spanning the repeats as described in Sundararajan et al. (2010) (primers and conditions are in the Supplemental Material). Colonies with the desired tract length were grown for six to seven cell divisions to allow expansion, contraction, or breakage and were plated on FOA-Leu or YC-Leu plates. For the instability assay, CAG repeat length in daughter colonies on the YC-Leu plates was assessed by PCR amplification and sizing by high-resolution gel electrophoresis in 100–200 daughter colonies from at least two transformants in at least three independent assays (Supplemental Table S4). To assay fragility, colonies growing on FOA-Leu and YC-Leu were counted, and a rate of mutation was calculated; at least three independent assays were performed per strain (Supplemental Table S3). A subset of FOA^R colonies was checked for YAC structure; end loss in FOA^R colonies occurred at a similar frequency in wild-type CAG-70 and the mutant strains studied (Supplemental Table S5).

ChIP

Cells with Myc-tagged proteins and CAG repeats (or no repeat control) were arrested in G1 with α factor, released into fresh medium, collected at the indicated time points, and processed as described in the Supplemental Material. Levels of input and immunoprecipitated DNA were analyzed by real-time PCR using primers that amplify a 168-bp region that is 92 bp from the repeat tract on chromosome VI or the *OLI1* mitochondrial locus (primers are listed in the Supplemental Material). Each ChIP was performed at least twice, and PCR reactions were run in duplicate. For normalization of each sample and time point, immunoprecipitated over input was used to calculate the absolute enrichment of the Myc-tagged protein at the long tract (CAG-130) or no tract (CAG-0) sequence or *OLI1* control locus using a standard curve for quantification.

Protein extraction, detection, and quantification

Yeast cells were grown to OD_{600} of 0.6–1.0, arrested with 10 μM α factor, and released into either YEPD or 0.03% MMS + 0.2M HU for 1 h. Cells (8×10^7) were harvested and processed as described in the Supplemental Material. Equal amounts of extracted proteins were diluted, separated, blotted, probed with the indicated antibody, detected, and quantified as described in the Supplemental Material. Rad52-SMT3 bands were normalized to the G6PDH bands run in the same lane on the same gel.

Acknowledgments

Thanks to Nathan Lingafelter for help with analyzing zoning data, and special thanks to Michael Lisby, Sue Jaspersen, Rodney Rothstein, and Hannah Klein for sharing reagents. This research was funded by Tufts University, National Institutes of Health grant P01GM105473 to C.H.F., a Tufts Graduate Student Research Award to X.A.S., and Swiss National Science Foundation grants and a Human Frontiers Science Program grant to S.M.G.

References

Altmannova V, Eckert-Boulet N, Arneric M, Kolesar P, Chaloupkova R, Damborsky J, Sung P, Zhao X, Lisby M, Krejci L. 2010. Rad52 SUMOylation affects the efficiency of the DNA repair. *Nucleic Acids Res* **38:** 4708–4721.

Bennett CB, Lewis LK, Karthikeyan G, Lobachev KS, Jin YH, Sterling JF, Snipe JR, Resnick MA. 2001. Genes required for ionizing radiation resistance in yeast. *Nat Genet* **29:** 426–434.

Bohm S, Mihalevic MJ, Casal MA, Bernstein KA. 2015. Disruption of SUMO-targeted ubiquitin ligases Slx5–Slx8/RNF4 alters RecQ-like helicase Sgs1/BLM localization in yeast and human cells. *DNA Repair (Amst)* **26:** 1–14.

Brohawn SG, Partridge JR, Whittle JR, Schwartz TU. 2009. The nuclear pore complex has entered the atomic age. *Structure* **17:** 1156–1168.

Burgess RC, Rahman S, Lisby M, Rothstein R, Zhao X. 2007. The Slx5–Slx8 complex affects sumoylation of DNA repair proteins and negatively regulates recombination. *Mol Cell Biol* **27:** 6153–6162.

Bystricky K, Van Attikum H, Montiel MD, Dion V, Gehlen L, Gasser SM. 2009. Regulation of nuclear positioning and dynamics of the silent mating type loci by the yeast Ku70/Ku80 complex. *Mol Cell Biol* **29:** 835–848.

Callahan JL, Andrews KJ, Zakian VA, Freudenreich CH. 2003. Mutations in yeast replication proteins that increase CAG/CTG expansions also increase repeat fragility. *Mol Cell Biol* **23:** 7849–7860.

Chiolo I, Minoda A, Colmenares SU, Polyzos A, Costes SV, Karpen GH. 2011. Double-strand breaks in heterochromatin move outside of a dynamic HP1a domain to complete recombinational repair. *Cell* **144:** 732–744.

Cleary JD, Tome S, Lopez Castel A, Panigrahi GB, Foiry L, Hagerman KA, Sroka H, Chitayat D, Gourdon G, Pearson CE. 2010. Tissue- and age-specific DNA replication patterns at the CTG/CAG-expanded human myotonic dystrophy type 1 locus. *Nat Struct Mol Biol* **17:** 1079–1087.

Cobb JA, Bjergbaek L, Shimada K, Frei C, Gasser SM. 2003. DNA polymerase stabilization at stalled replication forks requires Mec1 and the RecQ helicase Sgs1. *EMBO J* **22:** 4325–4336.

Daee DL, Mertz T, Lahue RS. 2007. Postreplication repair inhibits CAG.CTG repeat expansions in *Saccharomyces cerevisiae*. *Mol Cell Biol* **27:** 102–110.

Dion V. 2014. Tissue specificity in DNA repair: lessons from trinucleotide repeat instability. *Trends Genet* **30:** 220–229.
Dion V, Gasser SM. 2013. Chromatin movement in the maintenance of genome stability. *Cell* **152:** 1355–1364.
Dion V, Kalck V, Horigome C, Towbin BD, Gasser SM. 2012. Increased mobility of double-strand breaks requires Mec1, Rad9 and the homologous recombination machinery. *Nat Cell Biol* **14:** 502–509.
Dion V, Kalck V, Seeber A, Schleker T, Gasser SM. 2013. Cohesin and the nucleolus constrain the mobility of spontaneous repair foci. *EMBO Rep* **14:** 984–991.
Esta A, Ma E, Dupaigne P, Maloisel L, Guerois R, Le Cam E, Veaute X, Coic E. 2013. Rad52 sumoylation prevents the toxicity of unproductive Rad51 filaments independently of the anti-recombinase Srs2. *PLoS Genet* **9:** e1003833.
Follonier C, Oehler J, Herrador R, Lopes M. 2013. Friedreich's ataxia-associated GAA repeats induce replication-fork reversal and unusual molecular junctions. *Nat Struct Mol Biol* **20:** 486–494.
Fouche N, Ozgur S, Roy D, Griffith JD. 2006. Replication fork regression in repetitive DNAs. *Nucleic Acids Res* **34:** 6044–6050.
Freudenreich CH, Kantrow SM, Zakian VA. 1998. Expansion and length-dependent fragility of CTG repeats in yeast. *Science* **279:** 853–856.
Galanty Y, Belotserkovskaya R, Coates J, Jackson SP. 2012. RNF4, a SUMO-targeted ubiquitin E3 ligase, promotes DNA double-strand break repair. *Genes Dev* **26:** 1179–1195.
Gellon L, Razidlo DF, Gleeson O, Verra L, Schulz D, Lahue RS, Freudenreich CH. 2011. New functions of Ctf18-RFC in preserving genome stability outside its role in sister chromatid cohesion. *PLoS Genet* **7:** e1001298.
Heun P, Laroche T, Shimada K, Furrer P, Gasser SM. 2001. Chromosome dynamics in the yeast interphase nucleus. *Science* **294:** 2181–2186.
Horigome C, Oma Y, Konishi T, Schmid R, Marcomini I, Hauer MH, Dion V, Harata M, Gasser SM. 2014. SWR1 and INO80 chromatin remodelers contribute to DNA double-strand break perinuclear anchorage site choice. *Mol Cell* **55:** 626–639.
House NC, Yang JH, Walsh SC, Moy JM, Freudenreich CH. 2014. NuA4 initiates dynamic histone H4 acetylation to promote high-fidelity sister chromatid recombination at postreplication gaps. *Mol Cell* **55:** 818–828.
Ii T, Mullen JR, Slagle CE, Brill SJ. 2007. Stimulation of in vitro sumoylation by Slx5–Slx8: evidence for a functional interaction with the SUMO pathway. *DNA Repair (Amst)* **6:** 1679–1691.
Iraqui I, Chekkal Y, Jmari N, Pietrobon V, Freon K, Costes A, Lambert SA. 2012. Recovery of arrested replication forks by homologous recombination is error-prone. *PLoS Genet* **8:** e1002976.
Jakob B, Splinter J, Conrad S, Voss KO, Zink D, Durante M, Lobrich M, Taucher-Scholz G. 2011. DNA double-strand breaks in heterochromatin elicit fast repair protein recruitment, histone H2AX phosphorylation and relocation to euchromatin. *Nucleic Acids Res* **39:** 6489–6499.
Jankowski C, Nasar F, Nag DK. 2000. Meiotic instability of CAG repeat tracts occurs by double-strand break repair in yeast. *Proc Natl Acad Sci* **97:** 2134–2139.
Kalocsay M, Hiller NJ, Jentsch S. 2009. Chromosome-wide Rad51 spreading and SUMO-H2A.Z-dependent chromosome fixation in response to a persistent DNA double-strand break. *Mol Cell* **33:** 335–343.
Kerrest A, Anand RP, Sundararajan R, Bermejo R, Liberi G, Dujon B, Freudenreich CH, Richard GF. 2009. SRS2 and SGS1 prevent chromosomal breaks and stabilize triplet repeats by restraining recombination. *Nat Struct Mol Biol* **16:** 159–167.
Khadaroo B, Teixeira MT, Luciano P, Eckert-Boulet N, Germann SM, Simon MN, Gallina I, Abdallah P, Gilson E, Geli V, et al. 2009. The DNA damage response at eroded telomeres and tethering to the nuclear pore complex. *Nat Cell Biol* **11:** 980–987.
Kim JC, Mirkin SM. 2013. The balancing act of DNA repeat expansions. *Curr Opin Genet Dev* **23:** 280–288.
Lahiri M, Gustafson TL, Majors ER, Freudenreich CH. 2004. Expanded CAG repeats activate the DNA damage checkpoint pathway. *Mol Cell* **15:** 287–293.
Lambert S, Watson A, Sheedy DM, Martin B, Carr AM. 2005. Gross chromosomal rearrangements and elevated recombination at an inducible site-specific replication fork barrier. *Cell* **121:** 689–702.
Lambert S, Mizuno K, Blaisonneau J, Martineau S, Chanet R, Freon K, Murray JM, Carr AM, Baldacci G. 2010. Homologous recombination restarts blocked replication forks at the expense of genome rearrangements by template exchange. *Mol Cell* **39:** 346–359.
Lemaitre C, Grabarz A, Tsouroula K, Andronov L, Furst A, Pankotai T, Heyer V, Rogier M, Attwood KM, Kessler P, et al. 2014. Nuclear position dictates DNA repair pathway choice. *Genes Dev* **28:** 2450–2463.
Lin Y, Leng M, Wan M, Wilson JH. 2010. Convergent transcription through a long CAG tract destabilizes repeats and induces apoptosis. *Mol Cell Biol* **30:** 4435–4451.
Lisby M, Barlow JH, Burgess RC, Rothstein R. 2004. Choreography of the DNA damage response: spatiotemporal relationships among checkpoint and repair proteins. *Cell* **118:** 699–713.
Liu G, Leffak M. 2012. Instability of (CTG)n*(CAG)n trinucleotide repeats and DNA synthesis. *Cell Biosci* **2:** 7.
Liu Y, Kao HI, Bambara RA. 2004. Flap endonuclease 1: a central component of DNA metabolism. *Annu Rev Biochem* **73:** 589–615.
Loeillet S, Palancade B, Cartron M, Thierry A, Richard GF, Dujon B, Doye V, Nicolas A. 2005. Genetic network interactions among replication, repair and nuclear pore deficiencies in yeast. *DNA Repair (Amst)* **4:** 459–468.
Lopez Castel A, Cleary JD, Pearson CE. 2010. Repeat instability as the basis for human diseases and as a potential target for therapy. *Nat Rev Mol Cell Biol* **11:** 165–170.
Marini V, Krejci L. 2010. Srs2: the 'odd-job man' in DNA repair. *DNA Repair (Amst)* **9:** 268–275.
McMurray CT. 2010. Mechanisms of trinucleotide repeat instability during human development. *Nat Rev Genet* **11:** 786–799.
Meister P, Gehlen LR, Varela E, Kalck V, Gasser SM. 2010. Visualizing yeast chromosomes and nuclear architecture. *Methods Enzymol* **470:** 535–567.
Mine-Hattab J, Rothstein R. 2012. Increased chromosome mobility facilitates homology search during recombination. *Nat Cell Biol* **14:** 510–517.
Mirkin SM. 2006. DNA structures, repeat expansions and human hereditary disorders. *Curr Opin Struct Biol* **16:** 351–358.
Mizuno K, Lambert S, Baldacci G, Murray JM, Carr AM. 2009. Nearby inverted repeats fuse to generate acentric and dicentric palindromic chromosomes by a replication template exchange mechanism. *Genes Dev* **23:** 2876–2886.
Nagai S, Dubrana K, Tsai-Pflugfelder M, Davidson MB, Roberts TM, Brown GW, Varela E, Hediger F, Gasser SM, Krogan NJ.

2008. Functional targeting of DNA damage to a nuclear pore-associated SUMO-dependent ubiquitin ligase. *Science* **322:** 597–602.

Nagai S, Davoodi N, Gasser SM. 2011. Nuclear organization in genome stability: SUMO connections. *Cell Res* **21:** 474–485.

Oza P, Jaspersen SL, Miele A, Dekker J, Peterson CL. 2009. Mechanisms that regulate localization of a DNA double-strand break to the nuclear periphery. *Genes Dev* **23:** 912–927.

Pelletier R, Krasilnikova MM, Samadashwily GM, Lahue R, Mirkin SM. 2003. Replication and expansion of trinucleotide repeats in yeast. *Mol Cell Biol* **23:** 1349–1357.

Ragland RL, Patel S, Rivard RS, Smith K, Peters AA, Bielinsky AK, Brown EJ. 2013. RNF4 and PLK1 are required for replication fork collapse in ATR-deficient cells. *Genes Dev* **27:** 2259–2273.

Sacher M, Pfander B, Hoege C, Jentsch S. 2006. Control of Rad52 recombination activity by double-strand break-induced SUMO modification. *Nat Cell Biol* **8:** 1284–1290.

Samadashwily GM, Raca G, Mirkin SM. 1997. Trinucleotide repeats affect DNA replication in vivo. *Nat Genet* **17:** 298–304.

Saponaro M, Callahan D, Zheng X, Krejci L, Haber JE, Klein HL, Liberi G. 2010. Cdk1 targets Srs2 to complete synthesis-dependent strand annealing and to promote recombinational repair. *PLoS Genet* **6:** e1000858.

Savouret C, Garcia-Cordier C, Megret J, te Riele H, Junien C, Gourdon G. 2004. MSH2-dependent germinal CTG repeat expansions are produced continuously in spermatogonia from DM1 transgenic mice. *Mol Cell Biol* **24:** 629–637.

Sogo JM, Lopes M, Foiani M. 2002. Fork reversal and ssDNA accumulation at stalled replication forks owing to checkpoint defects. *Science* **297:** 599–602.

Sundararajan R, Freudenreich CH. 2011. Expanded CAG/CTG repeat DNA induces a checkpoint response that impacts cell proliferation in *Saccharomyces cerevisiae*. *PLoS Genet* **7:** e1001339.

Sundararajan R, Gellon L, Zunder RM, Freudenreich CH. 2010. Double-strand break repair pathways protect against CAG/CTG repeat expansions, contractions and repeat-mediated chromosomal fragility in *Saccharomyces cerevisiae*. *Genetics* **184:** 65–77.

Taddei A, Schober H, Gasser SM. 2010. The budding yeast nucleus. *Cold Spring Harb Perspect Biol* **2:** a000612.

Therizols P, Fairhead C, Cabal GG, Genovesio A, Olivo-Marin JC, Dujon B, Fabre E. 2006. Telomere tethering at the nuclear periphery is essential for efficient DNA double strand break repair in subtelomeric region. *J Cell Biol* **172:** 189–199.

Tittel-Elmer M, Alabert C, Pasero P, Cobb JA. 2009. The MRX complex stabilizes the replisome independently of the S phase checkpoint during replication stress. *EMBO J* **28:** 1142–1156.

Tsang E, Miyabe I, Iraqui I, Zheng J, Lambert SA, Carr AM. 2014. The extent of error-prone replication restart by homologous recombination is controlled by Exo1 and checkpoint proteins. *J Cell Sci* **127:** 2983–2994.

Usdin K, House NC, Freudenreich CH. 2015. Repeat instability during DNA repair: insights from model systems. *Crit Rev Biochem Mol Biol* **22:** 1–26.

Voineagu I, Freudenreich CH, Mirkin SM. 2009. Checkpoint responses to unusual structures formed by DNA repeats. *Mol Carcinog* **48:** 309–318.

Xie Y, Kerscher O, Kroetz MB, McConchie HF, Sung P, Hochstrasser M. 2007. The yeast Hex3.Slx8 heterodimer is a ubiquitin ligase stimulated by substrate sumoylation. *J Biol Chem* **282:** 34176–34184.

Yeager TR, Neumann AA, Englezou A, Huschtscha LI, Noble JR, Reddel RR. 1999. Telomerase-negative immortalized human cells contain a novel type of promyelocytic leukemia (PML) body. *Cancer Res* **59:** 4175–4179.

Yin Y, Seifert A, Chua JS, Maure JF, Golebiowski F, Hay RT. 2012. SUMO-targeted ubiquitin E3 ligase RNF4 is required for the response of human cells to DNA damage. *Genes Dev* **26:** 1196–1208.

Yoon SR, Dubeau L, de Young M, Wexler NS, Arnheim N. 2003. Huntington disease expansion mutations in humans can occur before meiosis is completed. *Proc Natl Acad Sci* **100:** 8834–8838.

Zellweger R, Dalcher D, Mutreja K, Berti M, Schmid JA, Herrador R, Vindigni A, Lopes M. 2015. Rad51-mediated replication fork reversal is a global response to genotoxic treatments in human cells. *J Cell Biol* **208:** 563–579.